
***Vibrio splendidus* O-antigen structure: A trade-off between virulence to oysters and resistance to grazers**

Oyanedel Daniel ¹, Labreuche Yannick ^{2,3}, Bruto Maxime ^{2,3}, Amraoui Hajar ¹, Robino Etienne ¹, Haffner Philippe ¹, Rubio Tristan ¹, Charrière Guillaume ¹, Le Roux Frédérique ^{2,3,*}, Destoumieux-Garzón Delphine ^{1,*}

¹ IHPE, Univ Montpellier, CNRS, Ifremer, Université de Perpignan Via Domitia; Montpellier, France

² Ifremer, Unité Physiologie Fonctionnelle des Organismes Marins, ZI de la Pointe du Diable, CS 10070; F-29280 Plouzané, France

³ Sorbonne Universités, UPMC Paris 06, CNRS, UMR 8227, Integrative Biology of Marine Models, Station Biologique de Roscoff, CS 90074; F-29688, Roscoff cedex ,France

* Corresponding authors : Frédérique Leroux, email address : frederique.le-roux@sb-roscoff.fr ; Delphine Destoumieux-Garzon, email address : ddestoum@ifremer.fr

Abstract :

A major debate in evolutionary biology is whether virulence is maintained as an adaptive trait and/or evolves to non-virulence. In the environment, virulence traits of non-obligatory parasites are subjected to diverse selective pressures and trade-offs. Here we focus on a population of *Vibrio splendidus* that displays moderate virulence for oysters. A MARTX (Multifunctional-autoprocessing repeats-in-toxin) and a type-six secretion system (T6SS) were found to be necessary for virulence toward oysters, while a region (*wbe*) involved in O-antigen synthesis is necessary for resistance to predation against amoebae. Gene inactivation within the *wbe* region had major consequences on the O-antigen structure, conferring lower immunogenicity, competitive advantage and increased virulence in oyster experimental infections. Therefore, O-antigen structures that favor resistance to environmental predators result in an increased activation of the oyster immune system and a reduced virulence in that host. These trade-offs likely contribute to maintaining O-antigen diversity in the marine environment by favoring genomic plasticity of the *wbe* region. The results of this study indicate an evolution of *V. splendidus* toward moderate virulence as a compromise between fitness in the oyster as a host, and resistance to its predators in the environment.

Introduction

Parasite virulence encompasses two features of a disease producing capacity, i) infectivity, *i.e.* the capacity to colonize a host and ii) the ability to cause damage in a host (Pirofski and Casadevall, 2012).

A major debate in evolutionary biology is whether virulence can evolve to non-virulence while maintaining the ability to provide other adaptive advantages (Bull and Luring., 2014; Alizon and Michalakis., 2015; Cressler *et al.*, 2016). On the one hand, as virulence affects host fitness, it may select for host resistance leading to a permanent non-virulence state. On the other hand, as a parasite evolves, it may counteract host resistance and maintain (or increase) virulence in a co-evolutionary arms race. For non-obligatory infectious agents, selection upon virulence traits will continue outside the host (Levin, 1996; Matz and Kjelleberg, 2005; Brown., *et al* 2012). This condition is exemplified by coincidental selection of bacterial genes involved in resistance to grazing in the environment and cytotoxicity to host immune cells, *e.g.*, the macrophage (Adiba *et al.*, 2010). However, experimental evolution in the context of single or multiple predators has revealed that the resultant bacterial resistance is frequently associated with an accompanying attenuation of virulence through pleiotropic

Accepted Article

effects on growth or infectivity (Friman *et al.*, 2009; Mikonranta., *et al* 2012; Friman and Buckling, 2014), extending the long-standing debate regarding virulence evolution. Indeed, in the environment, virulence traits can be subjected to a multitude of pressures, yet relevant theories lack empirical data on the mechanisms of virulence gene acquisition, maintenance or loss (Ferenci., 2016).

Species of *Vibrionaceae* (herein named vibrio) are marine heterotrophic bacteria that are ecologically and metabolically diverse members of planktonic and animal-associated microbial communities (Takemura *et al.*, 2014). The genus encompasses the well-studied human pathogen, *V. cholerae*, as well as some very important albeit less thoroughly characterized animal pathogens (Le Roux and Blokesch, 2018). Vibrio-associated diseases in *Crassostrea gigas* have been steadily rising over the past decade (Le Roux *et al.*, 2015) and this oyster species is now considered as a model in which to explore vibrio disease dynamics in wild animals (Le Roux *et al.*, 2016). Moreover vibrios have been subjected to population genetic analyses, which has allowed the delineation of functionally and genetically cohesive ecological populations (Cordero and Polz, 2014; Shapiro and Polz, 2014). This population genetic structure provides a framework for the mapping of disease properties, the analysis of vibrio ecological and evolutionary dynamics, and the interpretation of selective mechanisms. We previously showed that some vibrio populations are preferentially associated with oyster tissues compared to the surrounding water (Bruto *et al.*, 2017). Within the diverse Splendidus clade, virulence represents an ancestral trait that has been lost in several populations (Bruto *et al.*, 2018). We identified diverse loci that are necessary for virulence, resulting in population-specific mechanisms that converge to a common end: cytotoxicity to immune cells and immune evasion (Piel *et al.*, 2019; Rubio *et al.*, 2019). To date the non-virulence status of Splendidus-related strains has been related to gene loss (Bruto *et al.*, 2018); however, whether and why gene acquisition could result in virulence attenuation remains to be determined.

Here we focused on a population taxonomically assigned to the marine species *V. splendidus* and positively associated with oysters (Bruto *et al.*, 2017). All members of this population were isolated in Spring, before oyster disease events. This sampling approach precludes biases associated with the selection of bacterial genotypes encoding high virulence potential (Bruto *et al.*, 2017). We show that, while members of this population display moderate virulence, at least one strain is non-virulent. Two loci, a MARTX gene clusters and a type six secretion system (T6SS), were found necessary for virulence. A third locus (*wbe*), involved in O-antigen synthesis, distinguished between strains based on their combination of virulence and O-antigen structure. Gene inactivation within the *wbe* region resulted in increased virulence, competitive advantage and lower immunogenicity in oyster, whereas it suppressed protection against grazing by marine amoebae. Our results suggest that a conversion of O-antigen structure resulting from *wbe* genes shuffling is involved in a trade-off between resistance to environmental grazing and virulence to oysters.

Results

Despite the presence of two virulence loci, *V. splendidus* strains can show a relatively moderate virulence toward oysters.

We previously demonstrated the coincidence of vibrio ecological population delineation with virulence for oyster (Bruto *et al.*, 2018). Here we focused on three populations positively associated with oysters. Strains of *V. splendidus* (population #23), associated to healthy oysters in spring, were significantly less virulent (82.1 % mean survival rate 24 hpi, ANOVA, $p < 0.05$ and Tukey HSD test) than populations isolated from diseased oysters in the summer (Bruto *et al.*, 2017, 2018) (Fig. 1A). Moreover, contrasting

virulence phenotypes were observed between strains of *V. splendidus* #23 when generating Kaplan-Meier survival curves over 6 days (Fig. 1B). Indeed, only 40-60% of oysters injected with strains 4G4_4, 4D1_8 and 3T8_11 were alive at day 3, and generally remained viable until day 6. To contrast with *V. crassostreae* and *V. splendidus* #24 (Fig. 1A), we classify these strains as moderately virulent. By comparison, strain 4G1_8 had no significant effect on oyster survival (survival > 82 %, Log-rank p-value = 0,035, Bonferroni corrected for 10 comparisons) over the 6 days.

We performed comparative genome analyses between the moderately virulent strains (3T8_11, 4D1_8, 4G4_4) and the non-virulent strain (4G1_8) to investigate the genetic bases of this moderately virulent phenotype. A total of 419 genes were found to be specific to the moderately virulent strains (maxLrap > 0.8; identity > 60%) (Table S1). Among these genes, 38 clustered in two loci potentially involved in virulence. A first locus (*rtxACHBDE*, gene labels GV4G44_v1_300029 to 300034 in 4G4_4) encodes a putative toxin (MARTX, gene *rtxA*), a putative acyltransferase (*rtxC*), an uncharacterized protein (*rtxH*), and a putative type I secretion system (*rtxBDE*) (Fig. S1A). The MARTXs found in 3T8_11, 4D1_8, 4G4_4 (5,088 amino acids) show 97.88% identities with the MARTX found in *V. splendidus* strain ZS185 (Bruto *et al.*, 2018) and contain a core structure composed of two conserved regions at the amino- and carboxyl-termini, a cysteine-protease domain (CPD), a Ras/Rap1-specific endopeptidase (RRSP), an actin cross-linking domain (ACD), an α/β hydrolase (ABH) and two other cysteine-protease effector domains (MCF) (Fig. S1B). We assessed genetically the importance of the MARTX encoding gene for *V. splendidus* #23 virulence in strain 4G4_4 by inactivation of the *rtxA* (*rtxA-i*). Inactivation did not impair growth in culture media (Fig. S2) but increased significantly survival of infected oysters, from 71.7 % to 82.5 %, when determined 24 hpi ($p < 0.05$) (Fig. 2).

A second locus (GV4G44_v1_320001 to 320032 in 4G4_4) encodes a type VI secretion system (T6SS), a contact-dependent contractile nanomachine used by many Gram-negative bacteria as weapons against a variety of prokaryotic and eukaryotic organisms (Cianfanelli *et al.*, 2016). The locus (herein named T6SS_{4G4_4}) is organized into, at least, three operons containing genes involved in the structure and assembly of the contractile complex (Fig S3). Specifically, for the strain 4G4_4 next to the gene encoding a PAAR-motif protein (DUF4150 domain and 380 amino acid extension of unknown function), we identified a putative immunity system for nucleic acid degrading toxins. The putative effector (GV4G44_v1_320031 in 4G4_4) contains an AHH (Ala-His-His) nuclease domain found in bacterial polymorphic toxin systems (Zhang *et al.*, 2011). In many bacterial models, T6SSs are involved in killing competing bacteria (Cianfanelli *et al.*, 2016). Here, we did not observe inter-bacterial killing *in vitro* when using 4G4_4 as a predator and *E. coli* ML35p (Lehrer *et al.*, 1988) as a prey (Fig S8). This result suggests that this T6SS_{4G4_4} may not function in bacterial killing or are restricted to congeners. Alternatively, T6SS_{4G4_4} expression could be restricted to specific conditions such as oyster infection. We also tested whether T6SS_{4G4_4} could mediate toxicity toward eukaryotic cells. This showed that the three moderately virulent strains of *V. splendidus* #23, as well as the non-virulent strain 4G1_8, which lacks the T6SS_{4G4_4} were all significantly cytotoxic, as they induced 25.9 to 51.3% hemocyte lysis over 18 h (p<0.05), as opposed to 4.1% for the negative control *V. tasmaniensis* LMG20012^T (Fig S4A). Consistent with this observation, we found that inactivation of *vipA* in 4G4_4 (GV4G44_v1_320017), which encodes a component of the T6SS_{#23} contractile sheath, did not alter strain cytotoxicity, in contrast to the *vipA1-i* inactivation of T6SS_{chr1-LGP32} in *V. tasmaniensis* LGP32 (Fig. S4B). On the other hand, the 4G4_4 *vipA-i* mutant showed attenuated virulence, as determined by a significant increase in oyster survival after vibrio injection, from 71.7 % (wild-type 4G4_4) to 90.8 % (4G4_4 *vipA-i*), p<0.05

(Fig. 2). Hence, the presence of T6SS_{4G4_4} affects virulence in the oyster, although its molecular mechanisms and cellular target(s) remain to be determined.

Specific O-antigen structure antagonizes with *V. splendidus* virulence

The O-antigen is a highly diverse structure of the lipopolysaccharide (LPS) molecules, and is displayed at the outer surface of Gram-negative bacteria. In *V. splendidus*, the *wbe* region involved in O-antigen synthesis was previously shown to exhibit extensive genetic diversity (Wildschutte *et al.*, 2010). Here, we found that the moderately virulent strains of *V. splendidus* #23 presents a *wbe* region structure (GV4G44_v1_410010 to GV4G44_v1_370009 in 4G4_4) that highly differs from that of the strain 4G1_8 (Table 1). To assess the possible consequences of *wbe* genetic organization on O-antigen structure, we analyzed the electrophoretic profiles of the LPS expressed by four strains of *V. splendidus* #23. All LPS were of smooth type (Pupo and Hardy, 2007), as indicated by the typical ladder-like electrophoretic profiles of molecules containing different numbers of O-antigen repeating units (Raetz and Whitfield, 2002)(Fig. 3A). Short-chain molecular species containing only lipid A and core oligosaccharides migrated to the bottom of the gel, and were observed in all bacterial strains. However, several major differences were observed between the non-virulent strain 4G1_8 and the three moderately virulent strains (4G4_4, 3T8_11 and 4D1_8). First, the non-virulent 4G1_8 displayed an LPS of higher molecular weight with a lower number of monosaccharide residues per O-antigen repeating unit, as indicated by the tighter spacing between bands (Fig. 3A). Second, the LPS profile of all moderately virulent strains showed a prominent band of molecules of moderate size that may indicate the attachment to the core of a fixed number of O-antigen repeating units, or of an oligosaccharide side chain. In contrast to the polysaccharide moieties, no difference could be

evidenced in the Lipid A anchor, as determined by MALDI-TOF-MS (Fig S5). To determine the functional consequences of such distinct LPS structures, we compared the ability of *V. splendidus* #23 strains to bind to cytochrome C, a cationic molecule that binds to the negatively-charged membranes of bacteria (Saar-Dover *et al.*, 2012; Cullen *et al.*, 2015). Cytochrome C bound significantly more to the non-virulent 4G1_8 (80.8 %) than to the three moderately virulent strains, which all showed a similar degree of binding (25.3 to 34.6 %), $p < 0.001$ (Fig. 3B). This result strongly suggests that genetic diversity in the *wbe* region of *V. splendidus* #23 strains determines strain O-antigen structure, with consequences on the strain's ability to interact with macromolecules (Fig. 3B).

The importance of the *wbe* region for O-antigen synthesis and strain serotypes was further addressed genetically. To this aim, a gene encoding a glycosyltransferase (*epsE*, GV4G44_v1_370043 in 4G4_4) was inactivated in two strains. The LPS structure of the *epsE-i* mutant showed a reduced number of monosaccharides per repeating units (tighter spacing of the bands) as well as a higher molecular weight than the wild-type 4G4_4 (Fig. 3A), confirming that the *wbe* region determines the O-antigen profile. Moreover, *epsE* inactivation in strain 4G4_4 was sufficient to increase cytochrome C binding from 33.7% in the wild type strain 4G4_4 to 71.6% in *epsE-i* ($p < 0.001$) reflecting important changes in the bacterial surface properties. Identical phenotypes on O-antigen structure and binding capacity were obtained for the *epsE-i* mutant derived from another moderately virulent strain, 4D1_8 (Fig S6).

We next explored the effect of *epsE* inactivation on virulence. The *epsE-i* mutant was found significantly more virulent than the wild type strain 4G4_4 in oyster experimental infections. Indeed, oyster survival rate dropped from 71.7% when injected with wild type 4G4_4 down to 58.8% upon 4G4_4 *epsE-i* injection, $p < 0.05$ (Fig. 2). In addition, the *epsE-i* mutant showed a significant competitive advantage over their wild-type parents, 4G4_4 and 4G1_8 in oyster colonization, as indicated by competitive index values > 0.5 (Fig. 4A).

Because the O-antigen is a well-known determinant of bacterial immunogenicity (Chatterjee and Chaudhuri, 2011), we next asked whether the oyster immune response depended upon the O-antigen structure. Cells of 4G4_4 wild type and *epsE-i* mutant were injected into juvenile oysters after removing all traces of culture medium (potentially immunogenic). Oyster immune gene expression was then measured by RT-qPCR 2 hpi to capture the oyster's early response to infection. We selected 8 genes (IL 17-1, IL 17R, NFκB, MyD88, TNF-14, CgLBP, CgBPI, CgBigDef-1) involved in recognition, immune signaling and pathogen control that were previously shown to respond to vibrio infections (Gonzalez *et al.*, 2007; Rosa *et al.*, 2011; Rubio *et al.*, 2019; Sun *et al.*, 2019). Only genes encoding cytokines or involved in signaling pathways, namely IL 17-1, MyD88 and TNF-14, were significantly more induced by injection of the wild type 4G4_4 cells relative to an injection of sterile seawater (SSW) (Fig. 4B; Fig. S7). Interestingly none of these important immune pathways was significantly induced by the 4G4_4 *epsE-i* mutant at this early time point. Therefore, the LPS structure harbored by the moderately virulent strains appears as more immunogenic than that of the corresponding *epsE-i* mutant. This lower immunogenicity could be responsible for the higher competitiveness and virulence of the 4G4_4 *epsE-i* mutant in oyster experimental infections (Fig 2 and 4A).

Trade-off between immunogenicity and grazing resistance is mediated by O-antigen structure

As non-obligate parasites, vibrios can encounter a variety of hosts and predators in the marine environment. To determine whether the O-antigen structure of *V. splendidus* #23 affects other biotic interactions, we tested each strain's resistance to grazing by a marine amoeba isolated from the oyster environment (Robino *et al.*, 2019). The wild-type 4G4_4 was resistant to grazing by *Vannella* sp. AP1411, as indicated by a stable relative fluorescence of the bacterial strain up to ten days after the

beginning of the grazing experiment (Fig 5A). In agreement *Vannella* sp. AP1411 did not grow on a 4G4_4 grazing lawn (Fig 5B). In contrast, the *epsE-i* derivative was significantly grazed, as indicated by the decrease of the relative fluorescence down to 46.8% ($p < 0.05$) of the vibrio lawn (Fig 5A) and enabled a significant amoeba growth (407 cells/mm², $p < 0.05$) after 12 days (Fig 5B). The grazer-susceptible control *V. tasmaniensis* LMG20012^T was almost completely grazed in the same time span, giving rise to a significant level of amoeba growth at day 12 (651 cells/mm², $p < 0.05$) (Fig.5). Taken altogether, these results show that the LPS structure present in moderately virulent strains of *V. splendidus* #23 is protective against amoeba grazing but immunogenic during the interaction with oysters.

Discussion

In the environment, vibrios are exposed to a diversity of selective pressures, that may have effects on their virulence (Cui *et al.*, 2015; Shapiro *et al.*, 2016; Roig *et al.*, 2018; Sakib *et al.*, 2018; López-Pérez *et al.*, 2019) Here, we identified in a population of vibrios, trade-offs between traits needed for resistance to a grazer and traits involved in virulence to oysters. Illustrating the “conflicting selection hypothesis” (Mikonranta *et al.*, 2012), an O-antigen structure conferring resistance to predation by marine amoebae showed increased immunogenicity, and lower competitiveness and virulence in oysters, showing that selection in the outside-host environment might conflict with optimized pathogenicity.

V. splendidus population #23 has been previously described as preferentially associated with oyster tissues, suggesting that oysters represent a permissive habitat for this population. This is supported here by the ability of all tested strains to kill the oyster hemocytes and thus potentially evade the host

immune response. To date cytotoxicity toward the oyster hemocytes has been described as a common trait of virulent vibrios, although based on population specific molecular determinants (Piel *et al.*, 2019; Rubio *et al.*, 2019). The present study shows that dampening of oyster cellular defenses is a trait not restricted to virulent populations but shared by moderately and non-virulent strains that constitute the microbiota of healthy oysters.

Although less virulent than vibrios associated to disease (*V. splendidus* #24 and *V. crassostreae*), some *V. splendidus* #23 strains were able to affect oyster survival in experimental infections. This moderate degree of virulence results at least in part from the acquisition of two loci encoding effector delivery systems, a MARTX gene complex and a T6SS. The MARTX toxins are multifunctional effector cargo translocation, processing and delivery machines that can deliver functionally diverse cytopathic bacterial effectors to target eukaryotic cell (Satchell, 2015). In *V. splendidus* #23, MARTX effector domains are potentially involved in: i) modulation of small GTPases and manipulation of host cell signaling (RRSP); ii) disruption of cytoskeletal integrity (ACD) ; iii) inhibition of endocytic trafficking and autophagy (ABH) ; and iv) induction of apoptotic cell death (MCF) (Gavin and Satchell, 2015). The *V. splendidus* #23 MARTX share the same overall structure as *V. vulnificus* MARTX type III, *i.e.* an MCF domain, an ABH domain, and then a second copy of MCF follow the ACD domain. In *V. vulnificus* the MARTXs appear to be essential for protection both from fish phagocytic cells and from predation by amoeba (Lee *et al.*, 2013).

The T6SS nanomachines and its effectors are highly diverse in vibrios, acting against bacterial competitors (Unterweger *et al.*, 2014), amoeba or phagocytic cells during an intracellular stage (Ma *et al.*, 2009) or directly by contact with the target eukaryotic cell. Our cytotoxicity assays suggest that in *V. splendidus* #23, the T6SS does not target oyster hemocytes, in contrast to *V. tasmaniensis* or *V.*

crassostreae (Piel *et al.*, 2019; Rubio *et al.*, 2019). The presence of toxin and immunity modules in the T6SS loci would rather indicate anti-bacterial activity. However the T6SS might also be tightly regulated transcriptionally or post-translationally by lifestyle of the bacterium, or by membrane damage due to conjugation or membrane-targeting antibiotic (Ho *et al.*, 2013). Indeed a within-host restricted expression was previously observed in *V. tasmaniensis* for T6SS_{Chr2-LGP32}, one of the two chromosomal T6SS identified in this population (Rubio *et al.*, 2019). Future work should explore the environmental conditions necessary for its expression and function in order to formally demonstrate its role in inter-bacteria competition. Overall, the selection of specific effector domains within the T6SS or MARTX loci may arise as a result of the evolutionary arms race between bacteria, competitors and predators and could have correlative effects on bacterial virulence, hence supporting the “coincidental selection hypothesis” (Levin, 1996; Matz and Kjelleberg, 2005; Brown *et al.*, 2012).

Various biotic interactions can also lead to a trade-off on virulence (Friman *et al.*, 2009; Mikonranta *et al.*, 2012; Friman and Buckling, 2014). We showed here that the acquisition of genes involved in the synthesis of the LPS O-antigen confers a phenotype resistant to predation by an amoeba but results in a reduced virulence in the oyster. LPS is major components of the outer membrane in Gram-negative bacteria. These molecules are composed of a conserved lipid structure that is embedded in the outer membrane, and a polysaccharide referred to as the O-antigen (Raetz and Whitfield, 2002). O-antigen structures are highly variable across strains of a species (Seif *et al.*, 2019) and the *wbe* region was identified as a hypervariable locus in *V. splendidus*, contributing to structural variations of O-antigen (Wildschutte *et al.*, 2010). Wildschutte *et al.* observed extensive gene shuffling in the *wbe* region, which provides a means for O-antigen structure selection. However, they did not find any predominant serotype within hosts but conversely observed closely related serotypes, expressing the same O-antigen, among different hosts (Wildschutte *et al.*, 2010), which raises the questions about

whether/how the selection of O-antigen structures occurs outside the host. In nature this outer membrane structure directly interacts with ambient surfaces in the environment and, thus is subject to environmental selective pressures (Wildschutte *et al.*, 2004; March *et al.*, 2013). Indeed O-antigens constitute a first line of defense against predators (Simkovsky *et al.*, 2016) and have been shown to mediate antimicrobial resistance (Band and Weiss, 2015). Here we found that mutation of the *wbe* region was detrimental to the resistance of amoeba grazing. Indeed, a *V. splendidus* #23 lost its resistance upon mutation of the *wbe* region. Therefore, selective forces exerted by environmental predators may have favored the maintenance of this *wbe* encoded O-antigen structure.

In the host, O-antigens play a key role in both the activation of innate immunity and resistance to host immune effectors (Raetz and Whitfield, 2002). This dual function has important consequences on disease outcomes. In the rainbow trout (*Oncorhynchus mykiss*) pathogen *Vibrio anguillarum*, O-antigen polysaccharides were reported to determine the capacity to evade phagocytosis by skin epithelial cells (Lindell *et al.*, 2012). In *Vibrio vulnificus*, O-antigen polysaccharides are protective against serum complement, playing a key role in virulence for eels (Amaro *et al.*, 1997). Here, mutation of the *wbe* region yielded a modified O-antigen structure that significantly increased strain competitiveness and virulence. The O-antigen modification affected the polysaccharide structure and reduced strain immunogenicity, as indicated by the lack of induction of important oyster immune pathways involved in vibrio recognition (Rubio *et al.*, 2019) during early infection stages. This result indicates that strains of *V. splendidus* #23 with moderate virulence harbor an O-antigen structure easily recognized by the oyster immune system, leading to suboptimal colonization capacity. A trade-off between virulence and resistance to predators outside of host tissue was previously reported for *Salmonella enterica* O-antigen structure, which is under epigenetic control (Cota *et al.*, 2015). In this species, the O-antigen is a receptor for phage, and resistance is acquired by phase variation of O-

antigen chain length, *i.e.* phenotypic plasticity. Adaptations to phage predation involving trade-offs in evolutionary fitness and virulence have also been described for *V. cholerae*. Resistance to the lytic phage ICP2 results from mutations within either *ompU*, which encodes the major outer membrane porin, or its direct regulator *toxR* and results in virulence attenuation (Seed *et al.*, 2014).

Epidemiological success of non-obligate parasites depends on their environmental persistence in addition to the ability to produce major virulence factors. In complex microbial ecosystem such as the marine environment or the oyster microbiota, the outcomes for virulence trait selection can be positive (coincidental selection), neutral (relaxed selection), or negative (conflicting selection) (Mikonranta *et al.*, 2012). It has been argued that high virulence resulting in rapid killing of the host can be maladaptive as it does not allow parasite niche maintenance by the parasite (Alizon and Michalakis, 2015). Our genomic and phenotypic data suggest that *V. splendidus* #23 has evolved as a moderately virulent population with high fitness in its host, thereby supporting the theoretical prediction that moderate virulence can maximize parasite overall fitness (Alizon and Michalakis, 2015).

Experimental procedures

Strains, plasmid and primers

Vibrio strains used in this study were *V. splendidus* 3T8_11, *V. splendidus* 4D1_8, *V. splendidus* 4G1_8, *V. splendidus* 4G4_4 (Bruto *et al.*, 2018). *Vibrio* strains were cultured at 20°C in Luria Bertani medium (LB) supplemented with 0.5M NaCl (LBS). For *Vibrio splendidus* strains carrying either the integrative suicide plasmid pSW23T (Demarre *et al.*, 2005) or the pMRB-P_{LAC}GFP replicative plasmid (Le Roux *et al.*, 2011), the culture media were supplemented with 5µg/mL of Cm. For strains carrying a pMRB-P_{LAC}GFP replicative plasmid with a spectinomycin (Spc) resistance cassette, 100 µg mL⁻¹ Spc was used. *Escherichia coli* strains were cultured at 37°C in LB medium. Marine amoebae *Vannella* sp. AP1411 (Robino *et al.*, 2019) was grown for 3 days prior experiments at 18°C in 70% sterile seawater (70% SSW), using *E. coli* SBS363 as a nutritive source. Other strains, plasmids and primers used are included in Tables S2-S3-S4.

Animals

For experimental infections, we used *Crassostrea gigas* diploid oysters from a batch of standardized Ifremer spats (NSI) produced from a pool of 120 genitors. Animals were from both sexes. For hemocyte cytotoxicity assays, hemolymph was collected from adults (18 months old) produced from a pool of 120 genitors (ASI). All oysters were produced at the Ifremer hatchery in Argenton, France.

Experimental infections

Experimental infections were performed at 20 °C, as previously described (Rubio *et al.*, 2019). Juvenile oysters (1.5-2 cm) were anesthetized for 3 h. by immersion in seawater with 50 g L⁻¹ MgCl₂ (Suquet *et al.*, 2009). Stationary phase cultures (20 h. at 20°C with agitation at 150 rpm) were prepared for

Accepted Article

injection into the adductor muscle. For survival curves, two groups of 20 individuals were used. Each animal received an intramuscular injection of stationary phase culture (2×10^7 CFU per animal) or an equivalent volume of fresh culture medium. Each group of injected oysters was placed in a separate tank containing 3 L of seawater. Mortalities were monitored at 24h or daily for a 6-day period. The non-parametric Kaplan Meier test was used to estimate log-rank, including Bonferroni p-value correction for multiple comparison. Each phenotyping was repeated twice. For gene-expression analysis, stationary phase culture were washed three times in sterile seawater (SSW) and adjusted to 2×10^8 CFU/mL before injection into oyster adductor muscle. For each condition tested, 40 oysters were injected with 100 μ L of the washed bacterial culture or SSW only. 4 pools of 10 oysters were collected at time 0 (untreated controls) and at 2 h post injection (hpi) for each experimental condition. Pools of oyster tissues were snap frozen in liquid nitrogen and pulverized with a bead mixer mill (Retsch MM400). Pulverized pools were kept at -80 until RNA extraction. Experimental infections were performed according to the Ifremer animal care guidelines and policy.

Growth curves

Strains from -80°C stocks were plated on LB NaCl agar plates and incubated at 20°C for 24 h. Single colonies were used to seed LB NaCl broth. After overnight at 20°C with agitation at 150 rpm, cultures were adjusted to an OD₆₀₀ of 0,1 in fresh LB NaCl 0.5M broth. For each bacterial suspension, 300 μ L were disposed in triplicate in a 96 well platen and OD₆₀₀ was measured every 15 minutes in a TECAN infinite plate reader for 18 h.

Killing Assay

Vibrios strains were grown at 20°C in LBS media containing 5µg mL⁻¹ chloramphenicol when needed and *E. coli* ML35p was grown at 37°C in LB media containing 100 µg mL⁻¹ ampicillin.

Cultures of Predator and prey strains were normalized to an OD₆₀₀ of 1 and mixed at a MOI of 10. 50 µl of cell suspension were spotted on a 0.45 µm membrane (MF-Milipore™ MCE) placed in LBS agar to allow cell to cell contact and incubated at 20°C for 5 h. Filters were recovered and bacteria resuspended in LBS media. CFU of surviving *E. coli* per milliliter was determined by plating serial dilutions and selective growth at 37°C on LB agar containing 100 µg mL⁻¹ ampicillin.

Competitive index in mixed infections

For competitive assays of mix infections, adult oysters (ASI) were anesthetized and injected as described above with a 1:1 mixture of strains (2 x 10⁷ CFU total) in LB NaCl medium. 24 hpi, 8 oysters per group were sampled and homogenized with an ULTRA-TURRAX® homogenizer after adding 1 mL of SSW per g of flesh. Tissue homogenates were serially diluted in SSW and plated onto TCBS agar plates. Colonies were randomly selected after 48h at 20°C and tested by PCR with strain-specific primers (Table S4) to determine the ratio of strains present on each individual. Multiplex PCR with strain-specific primer couples 4G4_4F: 5'- TGCTATTGAGGAGGGACTGG-3'/4G4_4R: 5'- CACCTGAACCCAAAAATCGT-3' and 4G1_8F:5'-CAGAACTCTCTGGGCATGTG-3'/4G1_8R: 5'- AAAATCACACCCGACTCGAC -3', were used to discriminate between strains 4G4_4 and 4G1_8. To discriminate between 4G4_4 and 4G4_4**epsE*-i, the external primers used for mutant control Ext**epsE*-F: 5'- TCTCTGATGACTGCTCAACTG -3' and Ext**epsE*-R: 5'- TAAATAGACACGAAGGACCC -3' were used to identify *epsE*-i strains from wild type. To discriminate between 4G1_8 and 4G4_4 *epsE*-i

a first multiplex PCR was performed to differentiate between 4G4_4 and 4G1_8 strains and a second pcr with the *epsE-i* control primers to confirm that 4G4_4 identified colonies corresponded to *epsE-i* mutants. The competitive index was calculated as the ratio of the strains in the input inoculum over the ratio of the strains in the output obtained after 24 hpi. Competitive indices were then log transformed. Significant differences from a hypothetical value of 0 (no fitness advantage between strains) were determined with a one sample Student's t-test.

Molecular microbiology

Vibrio strains were grown at 20°C in LB NaCl medium. *Escherichia coli* strains were grown at 37°C in LB medium for cloning and conjugation experiments. Chloramphenicol (Cm) at 5 or 25 µg mL⁻¹ depending on the strain, Spectinomycin (Spc) at 100 ug mL⁻¹, thymidine (0.3 mM) and diaminopimelate (0.3 mM) were added as supplements when necessary. Conjugations between *E. coli* and *Vibrio* were performed at 30 °C as described previously (Le Roux *et al.*, 2007). Gene inactivation was performed by cloning ~ 500 bp of the target gene in pSW23T (Demarre *et al.*, 2005) and selecting on Cm (5 µg / mL) the suicide plasmid integration obtained by a single recombination (Le Roux *et al.*, 2009). Mutants were screened for insertion of the suicide vector by PCR using external primers flanking the different targeted sequence for plasmid insertion (Table S4). To label bacteria with fluorescent emission, strains were transformed with the pMRB plasmid containing the green fluorescent protein (*gfp*) gene known to be stable in *Vibrio spp* (Le Roux *et al.*, 2011) resulting in a constitutive expression from a P_{lac} promoter under chloramphenicol or spectinomycin selection.

Grazing assay and monitoring of amoeba growth

Accepted Article

To prepare the co-culture of GFP-expressing vibrios and amoebae, 1 mL of vibrio overnight culture (3×10^9 CFU / mL) was mixed with 100 μ L of a 3 day-old *Vannella* sp. AP1411 culture (5×10^5 cells / mL) resuspended in 70% SSW. For the control without amoeba, the vibrio culture was mixed with 100 μ L of 70% SSW. For grazing experiments, 500 μ L of 70% SSW containing 1% agar were deposited in the wells of a 24-well plate (transparent flat bottom). Each well was covered with 50 μ L of the mixed vibrio/amoeba cultures and let dry for 4 h at 20°C under a sterile laminar flow. The 24-well plates were then incubated at 18°C in a humid atmosphere. GFP fluorescence intensity was measured daily over 12 days using a TECAN plate reader (λ_{ex} 480 nm/ λ_{em} 520 nm). To estimate the effect of the amoebae grazing activity on the abundance of GFP-expressing vibrios, the fluorescence intensity of the wells containing amoebae was compared with the fluorescence of vibrios lawn without amoebae, and expressed as a ratio. Each condition was performed in technical triplicates, and the more representative experiment is depicted out of at least three independent experiments. Error bars represent the standard error of the mean \pm SD. Statistical analysis was performed using RM-ANOVA and Tukey's HSD comparison test.

The proliferation of *Vannella* sp. AP1411 was monitored at days 6, 9 and 12 in grazing assays. Amoebae were directly imaged by phase-contrast microscopy and enumerated in triplicate for each condition. Every experiment was performed in technical triplicates, and the more representative experiment is depicted out of at least three independent experiments. Error bars represent the \pm SD. Statistical analysis was performed using ANOVA, $p < 0.001$ and Tukey HSD test.

LPS isolation and molecular characterization

LPS were prepared from 4 L of stationary phase cultures of vibrios growth in LB NaCl 0.5M. Cultures were centrifuged at 1500 g for 20 min and bacterial pellets were washed with SSW before fixation with

2 % paraformaldehyde (18 h at 4°C). Fixed bacteria were centrifuged (3000g for 20 min) and washed twice with 0.1 M Phosphate Buffer Saline before shipping in dry ice to LPS Bioscience, University Paris Sud, 91400 Orsay France. LPS structures were characterized by electrophoresis and/or MALDI-TOF-MS by as described in (Trent et al., 2012). Briefly, Lipids A were isolated from lyophilized bacteria by mild acid hydrolysis followed by an extraction with an appropriate chloroform-methanol-water mixture. Bacterial lysates were treated with Proteinase K and loaded to a 4-15% polyacrylamide gel for electrophoresis. Gels were silver-stained. MALDI-TOF-MS analysis was performed in negative-ion [M-H]⁻ / linear mode. A purified lipid A from *Escherichia coli* was used as a standard for external calibration of *V. splendidus* lipids A mass-spectra.

RT -qPCR monitoring of immune gene expression

Total RNA was extracted from 10 mg of pulverized oysters using Direct-zol RNA extraction kit (Zymo research). cDNA was synthesized using M-MLV RT (Invitrogen Inc.) with 1 µg of RNA and 250 ng of random primers (Promega). Real-time qPCR was performed on 40 ng/µl of cDNA at the qPHd platform of qPCR in Montpellier with the Light-Cycler 480 System (Roche) and using the oyster gene specific primers (Table S4). Relative expression was calculated using the $2^{-\Delta\Delta C_q}$ method (Pfaffl, 2001) , with normalization to the *C. gigas* EF1- α (GenBank AB123066). One-way ANOVA followed by Tukey HSD test for multiple comparisons was used to analyze the data.

***In vitro* cytotoxicity assays**

Hemolymph was collected from the oyster adductor muscle sinus using a 2-mL ice cold-syringe equipped with a 23-G needle to prevent cellular aggregation. Hemocytes were counted in a KOVA[®]

Accepted Article

slide and plated onto 96 well-plates to create a cell monolayer (2×10^5 cells per well). After 1h at 20°C, plasma was removed and $5 \mu\text{g } \mu\text{l}^{-1}$ Sytox Green (Molecular Probes) diluted in 200 μl sterile seawater was added to each well. Cell-free hemolymph (plasma) was obtained by centrifugation (3,000g, 15 min, 4°C) and filtration through a 0,2 μm syringe filter. Vibrios were centrifuged and resuspended in the cell free plasma for opsonization (60 minutes at 20°C). The OD_{600} of the vibrio suspension was normalized in SSW to 1 (10^9 CFU mL^{-1}) and vibrio were added to the wells at a MOI of 50:1. Hemocytes were incubated at 20°C for 18 h after which the Sytox fluorescence was measured (λ_{ex} 480nm / λ_{em} 550nm) using a TECAN infinite microplate reader. Fluorescence intensity was compared to the total cytolysis determined in control wells where hemocytes were lysed by adding 0.1% Triton X-100. An ANOVA followed by a Tukey's HSD test was performed on the data.

Cytochrome C binding assay

Stationary phase cultures (20 h, 20°C, 150 rpm) were washed twice by centrifugation (1500g, 20°C) with 20 mM MOPS buffer (pH 7,2) supplemented with sucrose for a final osmolarity of 450 mOsm to make it compatible with the hyper saline environment of marine bacteria but to eliminate interfering charged salts. After washing by centrifugation (1500g, 20 min), bacterial pellets were suspended in MOPS sucrose buffer and the suspension was adjusted to an OD_{600} of 6. Cytochrome C solution was prepared in MOPS-Sucrose buffer to a concentration of 5 mg mL^{-1} . Then, 900 μL of bacterial suspension were placed in 1.5 mL polypropylene microcentrifuge tubes with 0.5 mg mL^{-1} cytochrome c. Tubes were incubated for 15 min at 20°C and then centrifuged at 6000g at room temperature for 15 min. The OD_{530} of the supernatants was measured in a TECAN microplate reader (300 μL transferred in triplicates).

to 96 wells plates). The percentage of bound cytochrome c to bacteria was calculated relative to the OD₅₃₀ value of a 0.5 mg/mL cytochrome c control solution not exposed to bacteria.

Acknowledgements. We warmly thank Prof. Edward G. Ruby (University of Hawai'i, USA) for critical reading of the manuscript. We thank Prof. Hervé Cottet from the *IBMM* (Montpellier, France), Dr. Jeremie Vidal-Dupiol and Dr. Yannick Gueguen from *IHPE* (Montpellier, France) as well as Dr. Agnès Delmas from the *CBM* (Orléans, France) for fruitful discussions. We are indebted to Marc Leroy from *IHPE* for precious technical assistance, to Dr. Martine Caroff and Dr. Alexey Novikov from *LPS biosciences* (Orsay, France) for lipopolysaccharide characterization, and to Philippe Clair at the qPHD platform/Montpellier genomix (Montpellier, France) for access to qPCR. We thank Bruno Petton, Matthias Huber and Jacqueline Le Grand from the Ifremer for providing standardized oyster spats for experimental infections and adults for cellular biology. This work was supported by the European Union's Horizon 2020 Research and Innovation Program Grant *Vivaldi* 678589; the CNRS, PEPS Blanc 2016 (project *Like Inhospitality*); CONICYT PFCHA/Doctorado En El Extranjero Becas Chile/2016-72170430 to D.O.; AMIBADAPT project funded by LABEX CeMEB; The Agence Nationale de la Recherche (Revenge project, ANR-16-CE32-0008-01) to F.L.R., and the University of Montpellier (Doctoral School Gaia; to E.R. and T.R.). This study is set within the framework of the "Laboratoires d'Excellence (LABEX)" Tulip (ANR-10-LABX-41).

Conflict of Interest

The authors declare that there are no conflicts of interests related to this work

References

- Adiba, S., Nizak, C., van Baalen, M., Denamur, E., and Depaulis, F. (2010) From grazing resistance to pathogenesis: The coincidental evolution of virulence factors. *PLoS One* **5**: 1–10.
- Alizon, S. and Michalakis, Y. (2015) Adaptive virulence evolution: the good old fitness-based approach. *Trends Ecol Evol* **30**: 248–254.
- Amaro, C., Fouz, B., Biosca, E.G., Marco-Noales, E., and Collado, R. (1997) The lipopolysaccharide O side chain of *Vibrio vulnificus* serogroup E is a virulence determinant for eels. *Infect Immun* **65**: 2475 LP – 2479.
- Band, V.I. and Weiss, D.S. (2015) Mechanisms of Antimicrobial Peptide Resistance in Gram-Negative Bacteria. *Antibiot (Basel, Switzerland)* **4**: 18–41.
- Brown, S.P., Cornforth, D.M., and Mideo, N. (2012) Evolution of virulence in opportunistic pathogens: Generalism, plasticity, and control. *Trends Microbiol* **20**: 336–342.
- Bruto, M., James, A., Petton, B., Labreuche, Y., Chenivesse, S., Alunno-Bruscia, M., et al. (2017) *Vibrio crassostreae*, a benign oyster colonizer turned into a pathogen after plasmid acquisition. *ISME J* **11**: 1043–1052.
- Bruto, M., Labreuche, Y., James, A., Piel, D., Chenivesse, S., Petton, B., et al. (2018) Ancestral gene acquisition as the key to virulence potential in environmental {*Vibrio*} populations. *ISME J* **12**: 2954–2966.
- Bull, J.J. and Luring, A.S. (2014) Theory and Empiricism in Virulence Evolution. *PLOS Pathog* **10**: e1004387.

Chatterjee, D. and Chaudhuri, K. (2011) Association of cholera toxin with *Vibrio cholerae* outer membrane vesicles which are internalized by human intestinal epithelial cells. *FEBS Lett* **585**: 1357–1362.

Cianfanelli, F.R., Monlezun, L., and Coulthurst, S.J. (2016) Aim, Load, Fire: The Type VI Secretion System, a Bacterial Nanoweapon. *Trends Microbiol* **24**: 51–62.

Cordero, O.X. and Polz, M.F. (2014) Explaining microbial genomic diversity in light of evolutionary ecology. *Nat Rev Microbiol* **12**: 263–273.

Cota, I., Sánchez-Romero, M.A., Hernández, S.B., Pucciarelli, M.G., García-Del Portillo, F., and Casadesús, J. (2015) Epigenetic Control of *Salmonella enterica* O-Antigen Chain Length: A Tradeoff between Virulence and Bacteriophage Resistance. *PLoS Genet* **11**: e1005667–e1005667.

Cressler, C.E., McLEOD, D. V, Rozins, C., VAN DEN Hoogen, J., and Day, T. (2016) The adaptive evolution of virulence: a review of theoretical predictions and empirical tests. *Parasitology* **143**: 915–930.

Cui, Y., Yang, X., Didelot, X., Guo, C., Li, D., Yan, Y., et al. (2015) Epidemic Clones , Oceanic Gene Pools , and Eco-LD in the Free Living Marine Pathogen *Vibrio parahaemolyticus*. *Mol Biol Evol* **32**: 1396–1410.

Cullen, T.W., Schofield, W.B., Barry, N.A., Putnam, E.E., Rundell, E.A., Trent, M.S., et al. (2015) Antimicrobial peptide resistance mediates resilience of prominent gut commensals during inflammation. *Science (80-)* **347**: 170 LP – 175.

Demarre, G., Guérout, A.M., Matsumoto-Mashimo, C., Rowe-Magnus, D.A., Marlière, P., and Mazel, D. (2005) A new family of mobilizable suicide plasmids based on broad host range R388 plasmid (IncW) and RP4 plasmid (IncP α) conjugative machineries and their cognate *Escherichia coli* host strains. *Res Microbiol* **156**: 245–255.

Ferenci, T. (2016) Trade-off Mechanisms Shaping the Diversity of Bacteria. *Trends Microbiol* **24**: 209–223.

Friman, V.-P. and Buckling, A. (2014) Phages can constrain protist predation-driven attenuation of *Pseudomonas aeruginosa* virulence in multienemy communities. *ISME J* **8**: 1820–1830.

Friman, V.-P., Lindstedt, C., Hiltunen, T., Laakso, J., and Mappes, J. (2009) Predation on multiple trophic levels shapes the evolution of pathogen virulence. *PLoS One* **4**: e6761.

Gavin, H.E. and Satchell, K.J.F. (2015) MARTX toxins as effector delivery platforms. *Pathog Dis* **73**: ftv092–ftv092.

Gonzalez, M., Gueguen, Y., Desserre, G., de Lorgeril, J., Romestand, B., and Bachère, E. (2007) Molecular characterization of two isoforms of defensin from hemocytes of the oyster *Crassostrea gigas*. *Dev Comp Immunol* **31**: 332–339.

Ho, B.T., Basler, M., and Mekalanos, J.J. (2013) Type 6 secretion system–mediated immunity to type 4 secretion system–mediated gene transfer. *Science (80-)* **342**: 250 LP – 253.

Lee, C.-T., Pajuelo, D., Llorens, A., Chen, Y.-H., Leiro, J.M., Padrós, F., et al. (2013) MARTX of *Vibrio vulnificus* biotype 2 is a virulence and survival factor. *Environ Microbiol* **15**: 419–432.

Lehrer, R.I., Barton, A., and Ganz, T. (1988) Concurrent assessment of inner and outer membrane

permeabilization and bacteriolysis in *E. coli* by multiple-wavelength spectrophotometry. *J Immunol Methods* **108**: 153–158.

Levin, B.R. (1996) The evolution and maintenance of virulence in microparasites. *Emerg Infect Dis* **2**: 93–102.

Lindell, K., Fahlgren, A., Hjerde, E., Willassen, N.-P., Fällman, M., and Milton, D.L. (2012) Lipopolysaccharide O-antigen prevents phagocytosis of *Vibrio anguillarum* by rainbow trout (*Oncorhynchus mykiss*) skin epithelial cells. *PLoS One* **7**: e37678–e37678.

López-Pérez, M., Jayakumar, J.M., Haro-Moreno, J.M., Zaragoza-Solas, A., Reddi, G., Rodriguez-Valera, F., et al. (2019) Evolutionary model of cluster divergence of the emergent marine pathogen *Vibrio vulnificus*: from genotype to ecotype. *MBio* **10**: e02852-18.

Ma, A.T., McAuley, S., Pukatzki, S., and Mekalanos, J.J. (2009) Translocation of a *Vibrio cholerae* type VI secretion effector requires bacterial endocytosis by host cells. *Cell Host Microbe* **5**: 234–243.

March, C., Cano, V., Moranta, D., Llobet, E., Pérez-Gutiérrez, C., Tomás, J.M., et al. (2013) Role of bacterial surface structures on the interaction of *Klebsiella pneumoniae* with phagocytes. *PLoS One* **8**: e56847.

Matz, C. and Kjelleberg, S. (2005) Off the hook - how bacteria survive protozoan grazing. *Trends Microbiol* **13**: 302–307.

Mikonranta, L., Friman, V.-P., and Laakso, J. (2012) Life history trade-offs and relaxed selection can decrease bacterial virulence in environmental reservoirs. *PLoS One* **7**: e43801.

Pfaffl, M.W. (2001) A new mathematical model for relative quantification in real-time RT-PCR.

Nucleic Acids Res **29**: e45–e45.

Piel, D., Bruto, M., James, A., Labreuche, Y., Lambert, C., Janicot, A., et al. (2019) Selection of *Vibrio crassostreae* relies on a plasmid expressing a type 6 secretion system cytotoxic for host immune cells. *Environ Microbiol* **0**:

Pirofski, L. and Casadevall, A. (2012) Q and A: What is a pathogen? A question that begs the point. *BMC Biol* **10**: 6.

Pupo, E. and Hardy, E. (2007) Isolation of smooth-type lipopolysaccharides to electrophoretic homogeneity. *Electrophoresis* **28**: 2351–2357.

Raetz, C.R.H. and Whitfield, C. (2002) Lipopolysaccharide Endotoxins. *Annu Rev Biochem* **71**: 635–700.

Robino, E., Poirier, A.C., Amraoui, H., Le Bissonnais, S., Perret, A., Lopez-Joven, C., et al. (2019) Resistance of the oyster pathogen *Vibrio tasmaniensis* LGP32 against grazing by *Vannella* sp. marine amoeba involves Vsm and CopA virulence factors. *Environ Microbiol* **n/a**:

Roig, F.J., González-candelas, F., Sanjuán, E., and Fouz, B. (2018) Phylogeny of *Vibrio vulnificus* from the analysis of the core-genome : implications for intra-species taxonomy. *Front Microbiol* **8**: 1–13.

Rosa, R.D., Santini, A., Fievet, J., Bulet, P., Destoumieux-Garzón, D., and Bachère, E. (2011) Big defensins, a diverse family of antimicrobial peptides that follows different patterns of expression in hemocytes of the oyster *Crassostrea gigas*. *PLoS One* **6**: e25594–e25594.

Le Roux, F., Binesse, J., Saulnier, D., and Mazel, D. (2007) Construction of a *Vibrio splendidus* mutant

lacking the metalloprotease gene *vsm* by use of a novel counterselectable suicide vector. *Appl Environ Microbiol* **73**: 777–784.

Le Roux, F. and Blokesch, M. (2018) Eco-evolutionary dynamics linked to horizontal gene transfer in *Vibrios*. *Annu Rev Microbiol* **72**: 89–110.

Le Roux, F., Labreuche, Y., Davis, B.M., Iqbal, N., Mangenot, S., Goarant, C., et al. (2011) Virulence of an emerging pathogenic lineage of *Vibrio nigripulchritudo* is dependent on two plasmids. *Environ Microbiol* **13**: 296–306.

Le Roux, F., Wegner, K.M., Baker-Austin, C., Vezzulli, L., Osorio, C.R., Amaro, C., et al. (2015) The emergence of *Vibrio* pathogens in Europe: Ecology, evolution and pathogenesis (Paris, 11-12 March 2015). *Front Microbiol* **6**: 1–8.

Le Roux, F., Wegner, K.M., and Polz, M.F. (2016) Oysters and *Vibrios* as a model for disease dynamics in wild animals. *Trends Microbiol* **24**: 568–580.

Le Roux, F., Zouine, M., Chakroun, N., Binesse, J., Saulnier, D., Bouchier, C., et al. (2009) Genome sequence of *Vibrio splendidus*: an abundant planctonic marine species with a large genotypic diversity. *Environ Microbiol* **11**: 1959–1970.

Rubio, T., Oyanedel, D., Labreuche, Y., Toulza, E., Luo, X., Bruto, M., et al. (2019) Species-specific mechanisms of cytotoxicity toward immune cells determine the successful outcome of *Vibrio* infections. *Proc Natl Acad Sci* **116**: 14238.

Saar-Dover, R., Bitler, A., Nezer, R., Shmuel-Galia, L., Firon, A., Shimoni, E., et al. (2012) D-Alanylation of lipoteichoic acids confers resistance to cationic peptides in group B *Streptococcus* by

increasing the cell wall density. *PLOS Pathog* **8**: e1002891.

Sakib, S.N., Reddi, G., and Almagro-Moreno, S. (2018) Environmental role of pathogenic traits in *Vibrio cholerae*. *J Bacteriol* **200**: 1–12.

Satchell, K.J.F. (2015) Multifunctional-autoprocessing repeats-in-toxin (MARTX) Toxins of Vibrios. *Microbiol Spectr* **3**:

Seed, K.D., Yen, M., Shapiro, B.J., Hilaire, I.J., Charles, R.C., Teng, J.E., et al. (2014) Evolutionary consequences of intra-patient phage predation on microbial populations. *Elife* **3**: e03497–e03497.

Seif, Y., Monk, J.M., Machado, H., Kavvas, E., and Palsson, B.O. (2019) Systems biology and pangenome of salmonella O-Antigens. *MBio* **10**: e01247-19.

Shapiro, B.J., Levade, I., Kovacicova, G., Taylor, R.K., and Almagro-moreno, S. (2016) Origins of pandemic *Vibrio cholerae* from environmental gene pools. *Nat Microbiol.* **2**:16240

Shapiro, B.J. and Polz, M.F. (2014) Ordering microbial diversity into ecologically and genetically cohesive units. *Trends Microbiol* **22**: 235–247.

Simkovsky, R., Effner, E.E., Iglesias-Sánchez, M.J., and Golden, S.S. (2016) Mutations in novel lipopolysaccharide biogenesis genes confer resistance to amoebal grazing in *Synechococcus elongatus*. *Appl Environ Microbiol* **82**: 2738–2750.

Sun, J., Wang, Lingling, Wu, Z., Han, S., Wang, Liyan, Li, M., et al. (2019) P38 is involved in immune response by regulating inflammatory cytokine expressions in the Pacific oyster *Crassostrea gigas*. *Dev Comp Immunol* **91**: 108–114.

Suquet, M., de Kermoisan, G., Araya, R.G., Queau, I., Lebrun, L., Le Souchu, P., and Mingant, C.

(2009) Anesthesia in Pacific oyster, *Crassostrea gigas*. *Aquat Living Resour* **22**: 29–34.

Takemura, A., Chien, D., and Polz, M. (2014) Associations and dynamics of Vibrionaceae in the environment, from the genus to the population level . *Front Microbiol* **5**: 38.

Unterweger, D., Miyata, S.T., Bachmann, V., Brooks, T.M., Mullins, T., Kostiuk, B., et al. (2014) The *Vibrio cholerae* type VI secretion system employs diverse effector modules for intraspecific competition. *Nat Commun* **5**: 3549.

Wildschutte, H., Preheim, S.P., Hernandez, Y., and Polz, M.F. (2010) O-antigen diversity and lateral transfer of the wbe region among *Vibrio splendidus* isolates. *Environ Microbiol* **12**: 2977–2987.

Wildschutte, H., Wolfe, D.M., Tamewitz, A., and Lawrence, J.G. (2004) Protozoan predation, diversifying selection, and the evolution of antigenic diversity in *Salmonella* *Proc Natl Acad Sci U S A* **101**: 10644 LP – 10649.

Zhang, D., Iyer, L.M., and Aravind, L. (2011) A novel immunity system for bacterial nucleic acid degrading toxins and its recruitment in various eukaryotic and DNA viral systems. *Nucleic Acids Res* **39**: 4532–4552.

Figure legends.

Figure 1. *V. splendidus* #23 shows moderate virulence in oyster experimental infections.

(A) Oyster survival was measured after injection with fifteen *Vibrio* strains representative of three ecological populations (x-axis). Strains from *V. splendidus* #23 have been isolated from healthy oysters in spring, while strains from *V. crassostreae* and *V. splendidus* #24 have been isolated from diseased oyster in summer. A dose of 10^7 CFU was injected intramuscularly to individual juvenile oysters and the percentage of survival was measured after 24 hours (y axis). A significantly higher oyster survival was observed for *V. splendidus* #23, which appeared less virulent than the two other populations tested, (ANOVA, $p < 0.05$ and Tukey HSD test). Experiment was performed in duplicate and repeated once. (B) Kaplan Meier survival curves were generated for four strains of *V. splendidus* #23 (2×10^7 CFU per oyster). Mortalities were counted daily in two tanks containing 20 oysters for 6 days. Significant difference in survival curves (Log-rank p-value=0.0016, Bonferroni corrected for 10 comparisons) was recorded for strains 4G1_8 (non virulent) and 4G4_4 (moderately virulent). Data are representative of two independent experiments.

Figure 2. Oyster mortality in response to experimental infection with *Vibrio* wild type (wt) strains and isogenic mutants.

The *rtxA*, *vipA* and *epsE* genes were inactivated in *V. splendidus* #23 strain 4G4_4. The wild type strains 4G4_4 (virulent) and 4G1_8 (non-virulent), and the 4G4_4 mutants were injected to 40 oysters (2.10^7 CFU per animal). Data represent the survival percentage measured 24h post injection in three independent experiments. Mean values are displayed \pm SD. Different letters indicate a significant difference between them (ANOVA, $p < 0.05$ and Tukey HSD test). The *rtxA-i* and *vipA-i* mutants are

attenuated (higher oyster survival) in contrast to the *epsE-i* mutant, which is more virulent than the wild type 4G4_4 strain (lower oyster survival).

Figure 3. Distinct gene contents in the *wbe* region are responsible for LPS variability in *V. splendidus* #23

A- Silver-stained 4-15% polyacrylamide gel of LPS extracted from bacterial stationary phase cultures. *Salmonella typhimurium* Ra (rough type LPS lacking O-antigen) and *Escherichia coli* O111B4 (smooth type LPS containing O-antigen polysaccharides) are included as references. All strains from *V. splendidus* #23 are smooth type (presence of O-antigen). Strain 4G1_8 shows an LPS profile distinct from the rest of *V. splendidus* #23. The main differences between strains are highlighted with roman numerals. I shows different sizes of the Lipid A -oligosaccharide core (low size bands). II and III show differences in the O-antigen structure both at intermediate (II) and high size (III and IV). The *epsE-i* mutant shows important modifications of the O-antigen structure. **B-** Cytochrome C binding unraveling the effect of O-antigen structure on the interaction of bacteria with macromolecules. The ability of bacterial strains to bind cytochrome C is displayed. Data represent mean values of 3 independent experiments \pm SD. Different letters indicate a significant difference (ANOVA, $p < 0.05$ and Tukey HSD test).

Figure 4. O-antigen structure influences bacterial fitness and immune recognition in oysters.

A- Competitive index (CI) between wild type strains and *epsE-i* mutant of *V. splendidus*. Randomly selected colonies isolated from injected animals were identified by PCR. The competitive index was calculated as the ratio of the strains in the input inoculum over the ratio of the strains in the output at

24 hpi. Each dot represents the \log_{10} of the CI obtained from colonies isolated from individual oysters. Means significantly higher than value 0 (t-test, $p < 0.01$) were considered as a competitive advantage of the strain. B- Relative expression of immune genes in response to *Vibrio* injection. 4 pools of 10 oysters were sampled 2 hours after being injected either with sterile seawater (SSW) or wild type (wt) and *epsE-i* mutant of *V. splendidus* (2×10^7 CFU/animal). RNA was extracted from the 4 pools. For each pools, RT-qPCR was performed on immune genes to determine their expression relative to the elongation factor 1 alpha (EF1- α). The $\Delta\Delta^{ct}$ method was used (Pfaffl, 2001). Data are presented as the mean \pm SD. Different letters indicate a significant difference between them (ANOVA, $p < 0.05$ and Tukey HSD test).

Figure 5. Resistance to grazing by marine amoeba is dependent on LPS structure.

A- Bacterial resistance to grazing by *Vannella* sp. 1411 was assessed for *V. splendidus* strains 4G4_4 and *epsE-i* by measuring the fluorescence of the GFP-expressing bacteria after contact with amoebae over 12 days. The strain *V. tasmaniensis* LMG20012T was used as a grazing-susceptible control. Results show the mean of three technical replicates \pm SD. Data are representative of three independent experiments. Different letters indicate a significant difference, $p < 0.001$ (RM-ANOVA). B- Amoeba growth was monitored at day 6, 9 and 12 by manual counting under phase light microscopy. Each condition was counted in three technical replicates. The results shown are representative of three independent experiments. For each time point, different letters indicate a significant difference (ANOVA, $p < 0.001$ and Tukey HSD test).

Figure S1. The *rtxA*CHBDE cluster in *V. splendidus* #23.

A- The figure shows gene replacement between non-virulent and moderately virulent strains leading to loss/acquisition of the MARTX encoding genes cluster. B- MARTX effector domains. The domain abbreviations are: Rtx = Repeats-in toxin; ACD = Actin Cross-linking Domain; ABH = α/β Hydrolase; MCF = Makes Caterpillars Floppy; RRSP = Ras/Rap1-specific endopeptidase; CPD = Cysteine Protease Domain (Satchell, 2015)

Figure S2. Growth curves of mutants versus wild type strains in LB NaCl medium.

Data show mean values of technical triplicates \pm SD.

Figure S3. Genetic organization of the T6SS cluster in *V. splendidus* #23.

The figure shows gene replacements (in blue) between non-virulent and moderately virulent strains leading to loss/acquisition of a chromosomal T6SS-encoding gene cluster. Genes in green are specifically found in the non-virulent strain 4G1-8. Genes in red are specifically found in virulent strains and contain the T6SS genes. The gene cluster of the virulent strains is present on two contigs (genes GV4G44_380041 - GV4G44_380047 and GV4G44_320001 - GV4G44_320044). From the complete genome of *V. tasmaniensis* LGP32, which contains the same gene cluster, we found that genes GV4G44_380047 and GV4G44_320001 (hatched red genes) form a single large gene that is splitted in our assemblies due to numerous repeats.

Figure S4. Strains of *V. splendidus* #23 are cytotoxic towards hemocytes.

Maximum cytotoxicity exerted by *V. splendidus* over oyster hemocytes *in vitro*. A hemocyte monolayer was exposed to vibrios at a MOI of 1:50 and the percentage of cell lysis was monitored by the SYTOX Green assay. (A) shows that the four strains of *V. splendidus* #23 are cytotoxic towards hemocytes.

Data are representative of five independent experiments. (B) shows that the *vipA-i* mutant derived from *V. splendidus* 4G4_4 does not show any attenuation of its cytotoxicity towards hemocytes, unlike the *vipA1-i* mutant derived from *V. tasmaniensis* LGP32. Data are representative of three independent experiments. Mean values of three technical replicates are displayed \pm SD. Identical letters indicate a non-significant difference (ANOVA, $p < 0.05$ and Tukey HSD test).

Figure S5. Lipid A inferred structure does not differ between strains 4G1_8 and 4G4_4.

(A) Data show the MALDI-TOF spectra of 4G1_8 and 4G4_4 Lipid A. MALDI-TOF-MS analysis was performed in negative-ion [M-H]⁻ / linear mode. A major Lipid A molecular species was observed at m/z 1740.1-1740.7, which by analogy with *V. cholerae* Lipid A could be attributed to a hexa-acyl (6 FA) molecular species (Hankins *et al.*, 2011, 2012), with one suggested exception *i.e.* the presence of non-hydroxylated 12:0 fatty acid at the secondary C3' position. As a consequence, no molecular species with Glycine substitution was found in either strain. Moreover, no substitution of phosphate groups with charged amino derivatives such as phosphoethanolamine or aminoarabinose could be inferred from our MS spectra. An additional peak, common to both strains was observed at m/z 1976.1-1977.4, which could be tentatively attributed to a hepta-acyl Lipid A molecular species (7 FA) carrying an additional 16:0 or 16:1 fatty acid. This molecular species appeared more intense in the virulent 4G4_4 than in the non-virulent 4G1_8. (B) Lipid A structure from *Vibrio cholerae* O1 adapted from Hankins *et al.* (2012), Fig.2. The upper panel shows the MALDI-TOF spectra of *V. cholerae* Lipid A with a major molecular species at m/z 1756.1. The lower panel shows the corresponding hexa-acyl molecular species (6 FA). Numbers indicate the number of carbons per acyl chain.

Figure S6. Inactivation of *epsE* in strains 4G4_4 and 4D1_8 generates the same O-antigen modifications and cytochrome C binding phenotype.

(a) SDS PAGE electrophoresis of LPS extractions from bacterial cultures in stationary phase. (b) Percentage of cytochrome C bound to the bacterial surface of wild type strains and *epsE-i* isogenic mutants. Data represent mean values of 3 independent experiments \pm SD. Different letters indicate a significant difference (ANOVA, $p < 0.05$ and Tukey HSD test).

Figure S7. Immune genes that do not respond to early infection by *V. splendidus*. 4 pools of 10 oysters were sampled 2 h after being injected either with sterile seawater (SSW) or vibrio strains (2×10^7 CFU per animal). RNA was extracted from the 4 pools. For each pool, RT-qPCR was performed on immune genes to determine their expression relative to the elongation factor 1 alpha (EF1- α). The $\Delta\Delta^{ct}$ method was used (Pffafli., 2001). Data are presented as the mean \pm SD. Different letters indicate a significant difference (ANOVA, $p < 0.05$ and Tukey HSD test).

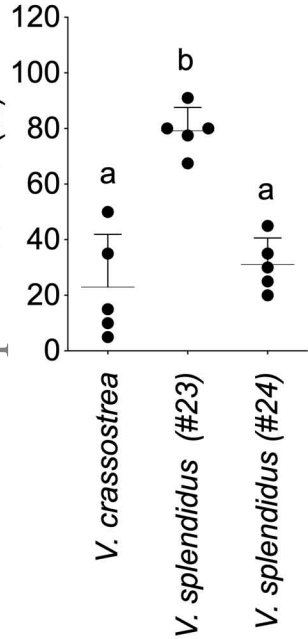
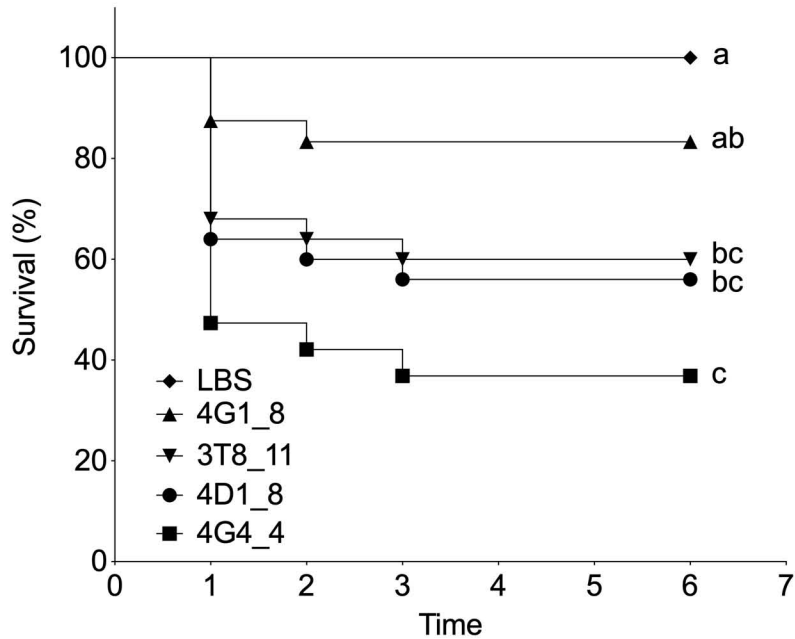
Figure S8. Strain 4G4-4 do not show killing activity against *E. coli* ML35p *in-vitro*. Cells were co-incubated in agar media for 4 h to allow cell to cell contact and T6SS mediated killing. Bars represent the mean CFU per milliliter of surviving *E. coli* from two replicates (\pm SD). Means were compared by a Student's t-test ^{ns}= $p > 0,05$

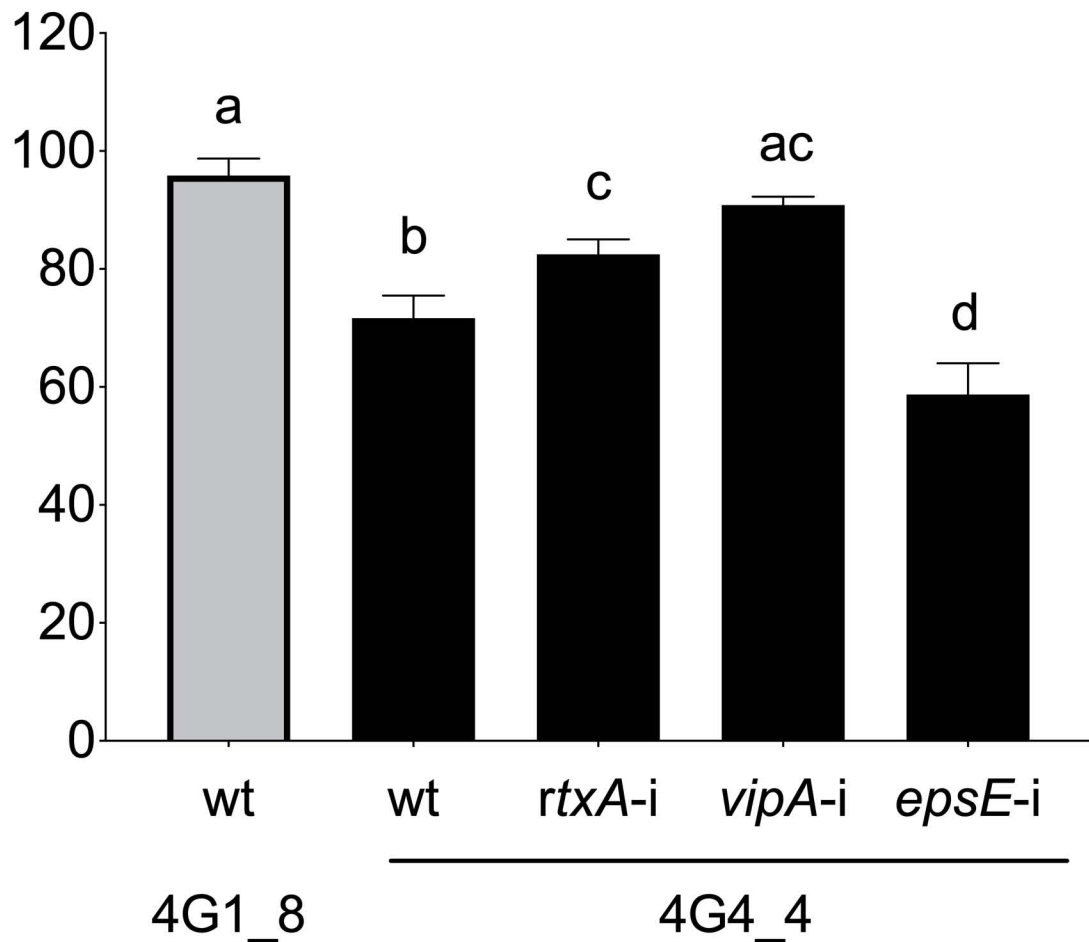
1 **Table 1. Gene content of the wbe regions from *V. splendidus* 4G4_4, 4G1_8, and *V. tasmaniensis* LGP32.** The *epsE* gene mutated in 4G4_4 appears in boldface.

2 Gene labels of strain 4G4_4 are used to represent the homolog genes of the moderately virulent strains of *V. splendidus* Pop#23

Pop#23			4G1_8			LGP32		
ORF#	Locus tag	Putative function or gene name	ORF#	Locus tag	% nt similarity	ORF#	Locus tag	% nt similarity
1	GV4G44_v1_410010	<i>gmhD</i>	1	GV4G18_v1_20068	97.4	1	VS_0201	94.9
2	GV4G44_v1_410009	UDP-glucose 6-dehydrogenase	2	GV4G18_v1_20067	94.8		–	
3	GV4G44_v1_410008	Transcriptional regulator	3	GV4G18_v1_20066	100	2	VS_0202	98.1
4	GV4G44_v1_410007	protein of unknown function	–	–	–	–	–	–
5	GV4G44_v1_410006	Peptidase	4	GV4G18_v1_20065	97.1	3	VS_0203	89.6
6	GV4G44_v1_410005	Serine acetyltransferase	5	GV4G18_v1_20064	100	4	VS_0204	100
7	GV4G44_v1_410004	NAD(P)H-glycerol-3-phosphate dehydrogenase	6	GV4G18_v1_20063	95.1	5	VS_0205	95.4
8	GV4G44_v1_410003	Export protein SecB	7	GV4G18_v1_20062	97.5	6	VS_0206	98.1
9	GV4G44_v1_410002	Rhodanese-related sulfurtransferase	8	GV4G18_v1_20061	99.3	7	VS_0207	100
10	GV4G44_v1_370056	protein of unknown function	–	–	–	–	–	–
11	GV4G44_v1_370055	GDP-mannose mannosyl hydrolase	–	–	–	–	–	–
12	GV4G44_v1_370054	mannose-1-phosphate guanyltransferase	–	–	–	–	–	–
13	GV4G44_v1_370053	Phosphomannomutase	–	–	–	–	–	–
14	GV4G44_v1_370052	GDP-D-mannose dehydratase, NAD(P)-binding	–	–	–	–	–	–
15	GV4G44_v1_370051	Bifunctional GDP-fucose synthetase	–	–	–	–	–	–
16	GV4G44_v1_370050	O-unit flippase	–	–	–	–	–	–
17	GV4G44_v1_370049	CDP-4-dehydro-6-deoxy-D-glucose 3-dehydratase (fragment)	–	–	–	–	–	–
18	GV4G44_v1_370048	Membrane protein of unknown function; putative O-antigen flippase	15	GV4G18_v1_20054	18.6	–	–	–
19	GV4G44_v1_370047	Putative glycosyl transferase family 11	–	–	–	–	–	–
20	GV4G44_v1_370046	Putative Uncharacterized glycosyltransferase HI_1578	–	–	–	–	–	–
21	GV4G44_v1_370045	Putative glycosyltransferase	37	GV4G18_v1_20032	26.5	–	–	–
22	GV4G44_v1_370044	Putative glycosyltransferase	–	–	–	–	–	–
23	GV4G44_v1_370043	Putative Glycosyl transferase, group 2 family <i>epsE</i>	–	–	–	–	–	–
24	GV4G44_v1_370042	Putative glycosyltransferase	13	GV4G18_v1_20056	29.2	–	–	–
25	GV4G44_v1_370041	O-antigen polymerase Wzy	–	–	–	19	VS_0220	22.3
26	GV4G44_v1_370040	Putative glycosyltransferase	12	GV4G18_v1_20057	37.3	–	–	–

27	GV4G44_v1_370039	UDP-GlcNAc:undecaprenylphosphate GlcNAc-1-phosphate transferase	18	GV4G18_v1_20051	81.1			
28	GV4G44_v1_370038	Regulator of length of O-antigen component of lipopolysaccharide chains	19	GV4G18_v1_20050	68.9			
29	GV4G44_v1_370037	Conserved membrane protein of unknown function				8	VS_0208	84
30	GV4G44_v1_370036	Outer membrane lipoprotein				9	VS_0209	95.7
31	GV4G44_v1_370035	Conserved hypothetical protein				10	VS_0210	85.3
32	GV4G44_v1_370034	Lipoprotein	22	GV4G18_v1_20047	20.3	11	VS_0212	93.9
33	GV4G44_v1_370033	<i>wza</i>	23	GV4G18_v1_20046	94.7	12	VS_0213	90.5
34	GV4G44_v1_370032	<i>wzb</i>	24	GV4G18_v1_20045	98.6	13	VS_0214	93.8
35	GV4G44_v1_370031	<i>wzc</i>	25	GV4G18_v1_20044	97.4	14	VS_0215	92.2
36	GV4G44_v1_370030	Conserved protein of unknown function	26	GV4G18_v1_20043	96.4			
37	GV4G44_v1_370029	protein of unknown function						
38	GV4G44_v1_370028	N-acetylmuramoyl-L-alanine amidase	29	GV4G18_v1_20040	91.8			
39	GV4G44_v1_370027	Conserved protein of unknown function	30	GV4G18_v1_20039	90.5			
40	GV4G44_v1_370026	Conserved protein of unknown function	32	GV4G18_v1_20037	71.8			
41	GV4G44_v1_370025	Conserved protein of unknown function	33	GV4G18_v1_20036	95.2			
42	GV4G44_v1_370024	HAD hydrolase, family IIA (fragment)						
43	GV4G44_v1_370023	HAD hydrolase, family IIA (fragment)						
44	GV4G44_v1_370022	protein of unknown function						
45	GV4G44_v1_370021	protein of unknown function						
46	GV4G44_v1_370020	putative CDP-glycerol:poly(Glycerophosphate) glycerophosphotransferase						
47	GV4G44_v1_370019	membrane protein of unknown function	35	GV4G18_v1_20034	24.6			
48	GV4G44_v1_370018	Family 2 glycosyltransferase						
49	GV4G44_v1_370017	membrane protein of unknown function						
50	GV4G44_v1_370016	conserved protein of unknown function						
51	GV4G44_v1_370015	putative glycosyl transferase, group 1	39	GV4G18_v1_20030	31.1			
52	GV4G44_v1_370014	Galactosyl-transferase	40	GV4G18_v1_20029	79.5	32	VS_0233	37.1
53	GV4G44_v1_370013	Putative acetyltransferase	41	GV4G18_v1_20028	89.9			
54	GV4G44_v1_370012	Perosamine synthetase (WeeJ)	42	GV4G18_v1_20027	93.6			
55	GV4G44_v1_370011	Mannosyl-transferase	43	GV4G18_v1_20026	96.3	33	VS_0234	89.2
56	GV4G44_v1_370010	Conserved protein of unknown function	44	GV4G18_v1_20025	98			
57	GV4G44_v1_370009	Phosphoglyceromutase	45	GV4G18_v1_20024	99.2	34	VS_0235	97.3

A**B**



A

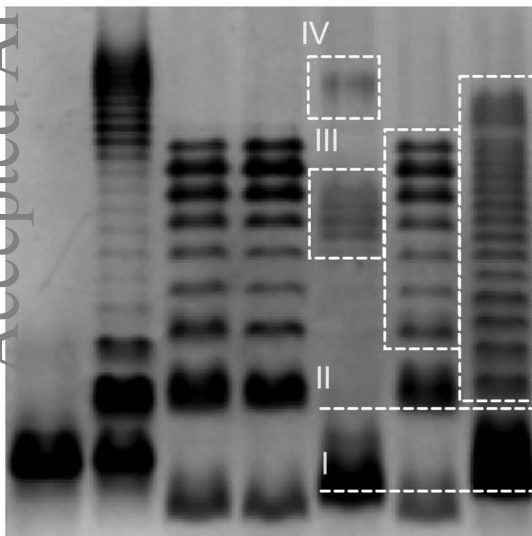
S. typhimurium Ra*E. coli* O111B4

3T8_11

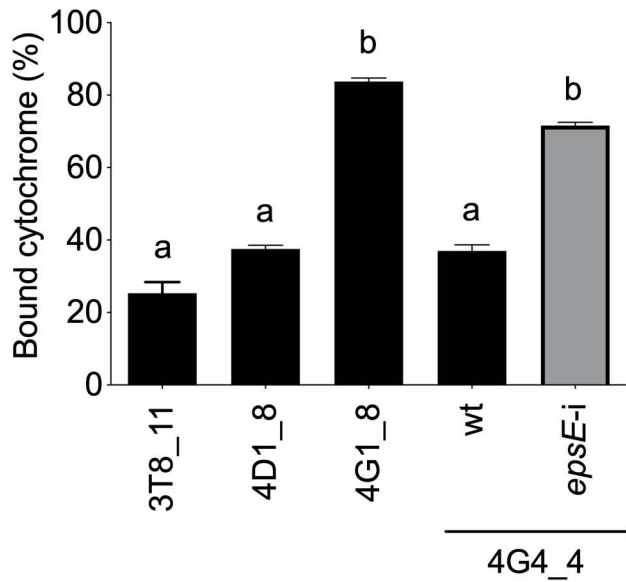
4D1_8

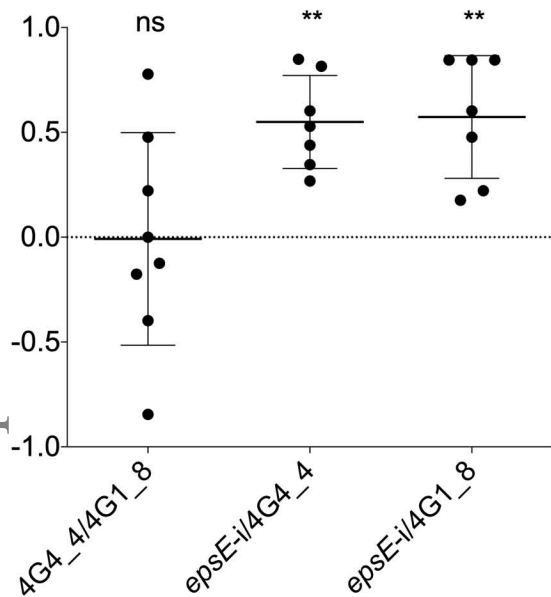
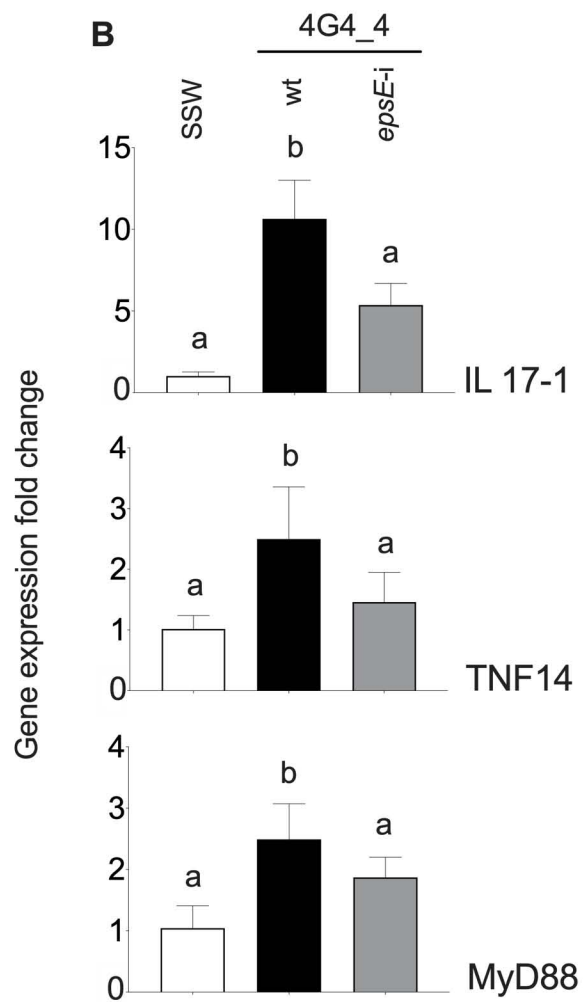
4G1_8

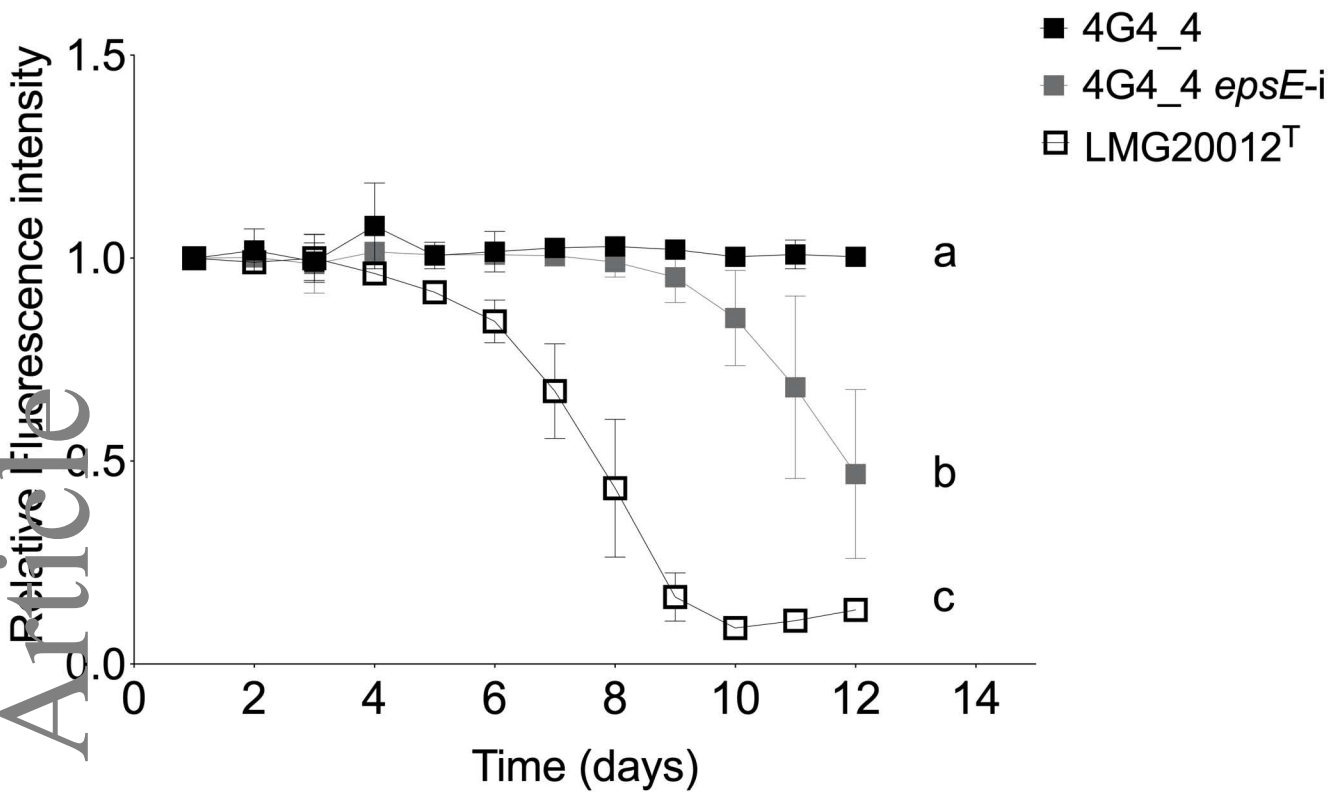
wt

epsE-i

B



A**B**

A**B**